UCRL-JC-131163
Preprint

MODELED NEAR-FIELD ENVIRONMENT POROSITY MODIFICATION DUE TO COUPLED THERMOHYDROLOGIC AND GEOCHEMICAL PROCESSES

John J. Nitao and William E. Glassley

This paper was prepared for submittal to
Scientific Basis for Nuclear Waste Management
Materials Research Society Symposium
Boston, Massachusetts, November 30–December 4, 1998

October 30, 1998

Lawrence
Livermore
National
Laboratory

MODELED NEAR-FIELD ENVIRONMENT POROSITY MODIFICATION DUE TO COUPLED THERMOHYDROLOGIC AND GEOCHEMICAL PROCESSES

John J. Nitao and William E. Glassley
Lawrence Livermore National Laboratory, P.O. Box 808, Livermore, CA 94551-9989

ABSTRACT

Heat deposited by waste packages in nuclear waste repositories can modify rock properties by instigating mineral dissolution and precipitation along hydrothermal flow pathways. Modeling this reactive transport requires coupling fluid flow to permeability changes resulting from dissolution and precipitation. Modification of the NUFT thermohydrologic (TH) code package to account for this coupling in a simplified geochemical system has been used to model the time-dependent change in porosity, permeability, matrix and fracture saturation, and temperature in the vicinity of waste-emplacement drifts, using conditions anticipated for the potential Yucca Mountain repository. The results show, within a few hundred years, dramatic porosity reduction approximately 10 m above emplacement drifts. Most of this reduction is attributed to deposition of solute load at the boiling front, although some of it also results from decreasing temperature along the flow path. The actual distribution of the nearly sealed region is sensitive to the time-dependent characteristics of the thermal load imposed on the environment and suggests that the geometry of the sealed region can be engineered by managing the waste-emplacement strategy and schedule.

INTRODUCTION

Transport of mass induced by thermally driven fluid flow is an important process in the Earth's crust [1, 2, 3, 4]. This transport is expressed as modifications in rock composition, changes in the assemblage of mineral species that are present, and alteration of porosity and permeability. It is now well established through experiments and simulation studies that thermally induced fluid movement will occur around the emplacement drifts at the proposed high-level nuclear waste repository at Yucca Mountain [5]. However, the mineralogical and physical changes associated with this TH system, and which geological evidence dictates will occur, have not been well characterized. This fact primarily reflects the historical limitations imposed by computational hardware and code development. The nonlinear, independent equations that describe thermal, hydrologic, and chemical processes have been known for some years [2, 3, 6]. However, the ability to couple these processes, taking into account changes in the permeability field as these processes evolve, has been restricted because of computer memory and processor limitations. Recent code developments and acquisition of high-performance computational hardware have allowed us to take the next step in developing this simulation capability, using a model that couples thermal, hydrologic, and geochemical processes in a computational framework that considers permeability evolution.

We report here the results of the first simulations in which these processes are coupled and applied to the thermohydrochemical (THC) evolution around waste-emplacement drifts. These simulations take into account the conditions anticipated for the proposed high-level nuclear waste repository at Yucca Mountain. The results demonstrate that fracture porosity will be irreversibly modified in the near vicinity of the waste-emplacement drifts, leading to the development of hydrologically sealed regions above and adjacent to the drifts. The actual geometry, rate of formation, and distribution of the altered rock are sensitive functions of the thermal loading and of the in situ effective surface areas of participating mineral phases.

PREVIOUS WORK

Extensive TH modeling of the potential high-level nuclear waste repository at Yucca Mountain [5, and references therein] has consistently demonstrated that a region of above-boiling temperatures around waste-emplacement drifts will develop. The extent, magnitude, and duration of these effects depend on thermal-loading strategies. Independently, numerous geochemical studies [7] have documented that changes in the mineralogy will occur under repository conditions. Although some effort has been made to examine the consequences of coupling these THC effects [8], these studies have been limited because the computational ability has not been available to simulate TH evolution under conditions where permeability is evolving.

MODEL DESCRIPTION

Physical Model

The model domain contains a single drift within a two-dimensional (2-D) columnar section of Yucca Mountain stratigraphy, which extends vertically from the water table to the ground surface. A dual-permeability model (DKM; see below) was used to model the 2-D fracture–matrix system.

The mineralogical system assumed that the rock consisted of a specified fraction of cristobalite and that the remainder of the rock being treated was inert. Phases also allowed to participate in the evolution of the system were quartz and amorphous silica. We discuss here only those simulations considering the cristobalite–quartz system. Mass action expressions were developed for dissolution and precipitation of these minerals and for the aqueous species present in this system. This system, albeit simplified, considers the volumetrically dominant phases expected to participate in reactive transport in the vicinity of the potential repository. Simulations involving a wide range of other mineral species are currently underway.

Although numerous scenarios were simulated, we present here two thermal loading scenarios to illustrate significant effects. In Case 1 (“Point-Load Scenario”), nominal design characteristics include an approximately 5 m, end-to-end spacing between waste containers, a 28 m spacing between emplacement drifts, no backfill, and an infiltration flux of 16 mm/yr. In Case 2 (“Line-Load Scenario”), the conditions were the same, except that the end-to-end spacing between containers was reduced to 10 cm and the spacing between emplacement drifts was doubled (to 56 m). Other conditions examined included variation in the infiltration flux and variation in the effective surface area of the dissolving phase.

Computational Model

All of the calculations described here have been accomplished using a modified version of the NUFT code [9]. The TH component of the model represents both heat flow and multiphase (gas- and aqueous-phase) flow and transport of chemical species, including air and water. Explicit account is taken of the following: thermal conduction in the bulk rock and in drift materials (including the dependence of rock thermal conductivity K_{th} on liquid-phase saturation S_{liq}); liquid-phase convection for saturated and unsaturated conditions; thermal radiation between all surfaces in the emplacement drift; gas-phase convection in the unsaturated zone, including that arising from barometric pumping, decay-heat-driven, buoyant, gas-phase convection, and decay-heat-driven boiling; liquid-phase species-diffusion in the unsaturated and saturated zone; binary gas-phase diffusion of air and water vapor in the unsaturated zone; and latent-heat effects that arise from the changes in thermal energy from the condensation of water vapor and the evaporation of liquid water.

The temperature-dependent, heat-capacity approach is not required because the influence of evaporation, latent-heat transport, and condensation is explicitly accounted for.

The geochemical component of the model uses a first-order, surface-area–dependent reaction rate (mol/s-m) formula to represent dissolution and precipitation of cristobalite and quartz, where the rate-constant temperature dependence was given by an Arrhenius relation. Mineral surface areas used in the rate law were developed by assuming spherical grains 10 microns in diameter and assuming that the effective surface area equated to the geometric surface area multiplied by the mineral fraction.

Temperature dependence of the equilibrium constants for the dissolution and precipitation reactions were treated as exponential functions.

The transport equation for silica was

$$\frac{\partial \phi \rho_1 S_1 \omega_\gamma}{\partial t} + \nabla \cdot \left[\omega_\gamma \mathbf{q}_1 - \phi S_1 \rho_1 \tau_1 D_\gamma \nabla \omega_\gamma \right] = -M r_\gamma$$

where t is time (s), ϕ is porosity, ω is the mass fraction of silica phase γ, S_l is the liquid phase saturation, ρ_l is the liquid phase mass density (kg/m^3), $\mathbf{q}_l$ is the specific liquid phase mass flux (kg/m^2), τ_l is the liquid phase tortuosity factor, $D\gamma$ is the diffusion coefficient (m^2/s), M is the molecular mass of silica (kg/mol), and $r\gamma$ is the reaction rate for phase γ.

The porosity change was treated as a linear function of the molar volume changes in the mineral phases.

The DKM treats the matrix and the fractures as two distinct porous continua, with transfer terms to represent the mass and heat flux between them. The DKM does not assume capillary-pressure equilibrium between fracture and matrix continua, allows thermodynamic disequilibrium between matrix blocks and the adjoining fractures, and allows for gas-phase pressure P_{gas} disequilibrium between the matrix blocks and adjoining fractures. Capillary pressure in the fracture and matrix continua was assumed to scale inversely with the porosity. The intrinsic permeabilities in the fracture and matrix continua were assumed to scale as the cube of the porosity.

The van Genuchten formula was used for the capillary pressure and relative permeability curves of the fracture and matrix. The residual saturation and the van Genuchten m parameters for capillary pressure and relative permeability curves were kept fixed with respect to changes in porosity. The hydrologic parameter values used were primarily from the Yucca Mountain July 1997 Total System Viability Performance Assessment—Viability Study (TSPA-VA) base case.

Mathematical Formulation and Computational Strategy

The balance equations for mass-transfer—including dispersive and diffusive fluxes, Darcy's law, and heat transfer—are discretized in space using the integrated finite-difference method and discretized in time using the fully implicit, backward Euler method. All three partial differential equations are fully coupled. The resulting nonlinear system of equations is solved at each time step using the Newton–Raphson method.

The methods for solving the system of linear equations generally are (1) the direct-solution method using D4 ordering or (2) the preconditioned, conjugate gradient method with various preconditioning schemes, including incomplete ILU with D4 or natural ordering.

The primary solution variables predicted by the model are fluid pressure, mass fraction of water vapor in the gas phase, liquid-phase saturation, and temperature. For DKM problems, the set of equations is repeated for each continuum, with simultaneous solution of the matrix and fracture sets.

For solute transport calculations, local thermodynamic equilibrium is assumed in the fluid phase, and partition coefficients are used for calculating the transfer of species between fluid phases and between fluid and solid phases.

The coupled TH and reactive-transport equations are solved by the NUFT code [9] in a sequential manner because this manner provides computational efficiency. In each solution cycle, the TH equations are solved over a single time step. The resulting temperature and flow fields are then used to solve the reactive-transport equations, using time steps that are equal to or smaller than the TH time step. Smaller time steps are used because time constants for reactive transport are often smaller than those for thermohydrology. Time-linear interpolated values based on the beginning and the end of the TH step are used for the flux $\mathbf{q}_l$, mass density ρ_l, saturation S_l, and temperature T fields in the reactive-transport model. The reactive-transport model is solved in this manner until it reaches the end time of the TH step. The simulation then passes the calculated porosity field to the TH component, which begins its next time step. The cycle is repeated until the ending simulation time is reached. Both the TH and reactive-transport models have automatic time-stepping for controlling the changes in the solution variables. For this simulation, the transport time steps were about an order of magnitude smaller than the TH time steps.

RESULTS

The results of the simulations demonstrate that porosity modification is a nearly irreversible, complex, time-dependent, and space dependent function of the heating scenario (Figure 1). Although a time series "movie" of the 2-D evolution of the porosity within approximately 50 m of the drift has been developed, to compare the porosity evolution under different heating conditions, we consider only three locations in the vicinity of a waste-emplacement drift: The first ("15 m Above" in Figure 1) is located within the area where heat-pipe properties develop, but is a significant distance from the emplacement drift (15 m from the waste package, ~12 m from the drift crown). The second ("6 m Above" in Figure 1) is located within a few meters of the drift crown and 6 m from a waste package. The third ("2 m From Wall" in Figure 1) is located at the same elevation as the waste package, ~2 m into the rock from the drift wall.

At the far location, 15 m above the waste package (WP), the nature of the porosity modification clearly depended on the heating scenario. For the point-load (PL) case, porosity continuously and slowly increased for the 20,000 yr of the simulation, reaching an enhancement of approximately 10%. This reflected primarily the effect of condensate dissolution on the *in situ* fracture mineralogy. For the line-load (LL) case at this location, the porosity quickly dropped to about 85% of its original value. This reflected primarily a greater localized heat load with its associated vigorous heat pipe extending some distance from the emplacement drift. The consequence was rapid deposition of silica at the boiling front as it sweeps past this location. Within a few hundred years, this condition stabilized, the heat pipe contracted, the porosity slowly began to recover, and values near 95% by 20,000 yr were achieved as undersaturated waters began to affect the earlier precipitated minerals.

At the location near the crown of the drift ("6 m Above" in Figure 1), both heating scenarios resulted in nearly complete elimination of fracture porosity within a few thousand years. The initial fracture permeability at the repository unit was 9.1×10^{-10} m^2. In the precipitation cap, the permeability had decreased to about 10^{-14} m^2. The rate at which this was achieved was strongly scenario-dependent, taking more than twice as long for the LL case than for the PL case. In addition, the LL case had an early period of porosity enhancement, reflecting the impact of flow of undersaturated waters and dissolution associated with short flow-path lengths early in the heating cycle.

Adjacent to the drift wall, significant fracture sealing occurred in both cases, after several thousand years, diminishing by 70% (LL case) to 50% (PL case). This sealing was due to cooling of fluids as they drained from warmer regions. Prior to sealing, no change occurred for the PL case, while the LL case experienced enhanced porosity as heated, undersaturated solutions drained down through that location.

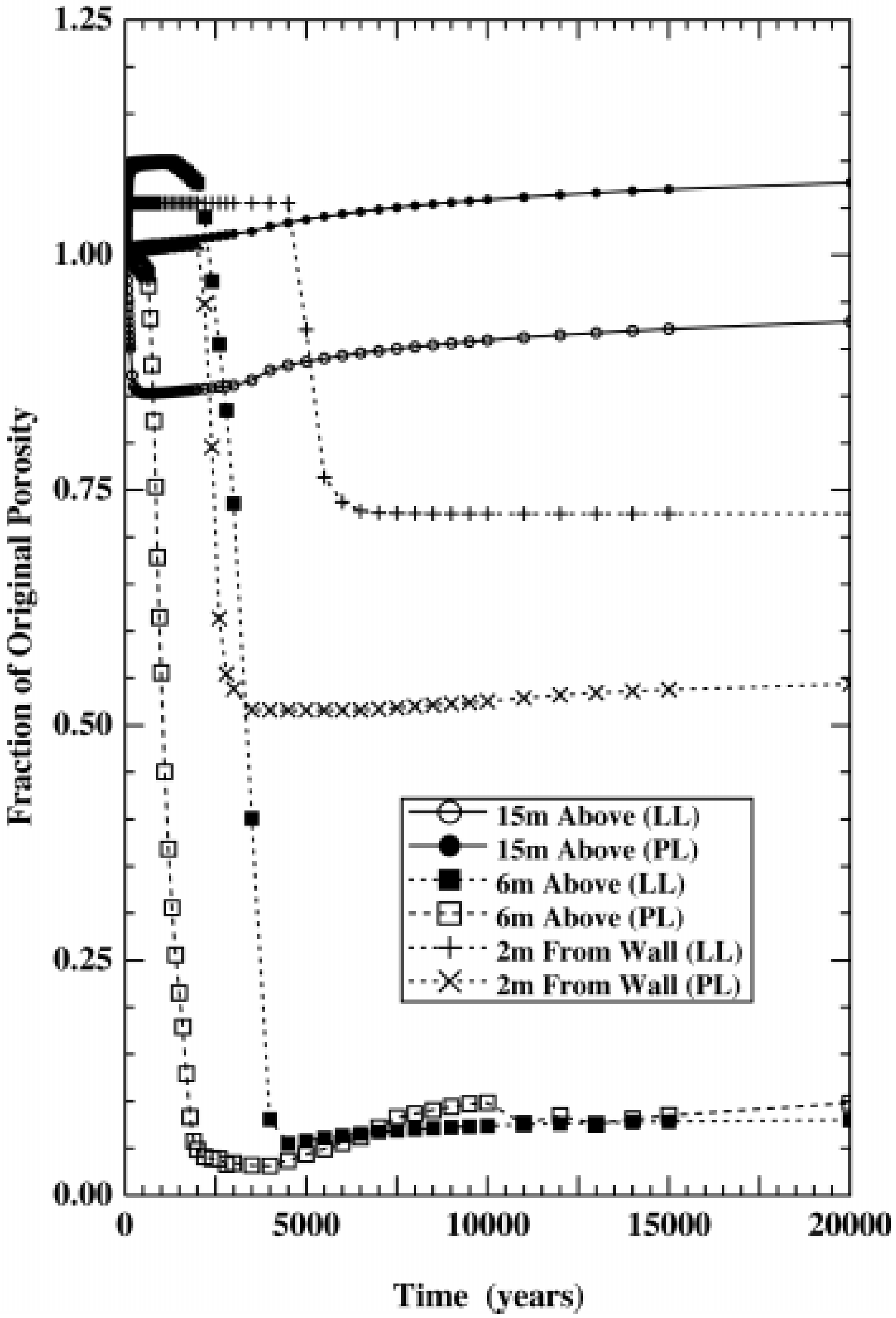

Figure 1. **Time dependent evolution of porosity at three locations in the vicinity of an emplacement drift. Results for both point load (PL) and line load (LL) scenarios are indicated.**

In both cases, a virtually sealed helmet formed around the top and sides of the drift, the extent and timing of which was crucially dependent on the specific heating scenario. For the PL case, this sealing tended to occur faster and tended to form a thicker zone within the rock adjacent to the drift walls. The LL scenario, on the other hand, formed a slightly thicker zone in the cap region, but required more time to do so. These differences demonstrate that temperature evolution is the significant determiner of rate and extent of silica-sealing of fractures. A PL WP distribution resulted in a smaller region of above-boiling conditions around the drift, and the boiling point isotherm collapsed back on the drift earlier than it did for the LL case.

The effect of surface area on the results was also considered by using surface area values that differed by several orders of magnitude. It was found, as expected, that increasing the surface area significantly (>10 times) dramatically increased the rate of formation and extent of sealing. The effect of infiltration flux was primarily to modify the geometry and extent of the boiling region, but the overall effect on the sealing process was small.

DISCUSSION AND CONCLUSIONS

These results demonstrate that porosity-reduction by silica deposition will modify hydrologic properties of the rock mass in the vicinity of waste-emplacement drifts. The time-dependent nature of these changes is complex. Periods of porosity reduction or enhancement can be followed by periods that reverse the nature of the change in porosity, depending upon heating histories and loading. These changes are of large magnitude and irreversible. Although the chemical system presented here is simplified, it likely represents a lower bound for the extent and magnitude of porosity reduction; with more complex chemistry, a wide range of mineral species with much larger molar volumes are likely to precipitate over a greater range of temperature and saturation conditions.

The parameters that exert the greatest control over mineral precipitation are temperature evolution and effective surface area. The former is an engineered property of the system and has the potential to be used to engineer the location and extent of mineral precipitation. The latter is an intrinsic, and variable, property of the rock system and needs to be better characterized to develop detailed, high-resolution models of high confidence.

The consequences of these results to repository performance may be substantial. Reduction in fracture aperture around the drifts may lead to reduced seepage into the drifts. However, the actual three-dimensional geometry of the sealed regions may be complex and uneven because of local inhomogeneity in hydrologic properties and mineral distributions along fractures. As a consequence, “dimples” in the sealed zone may possibly lead to perched condensate in some locations. Moreover, precipitation in the fractures will tend to be more extensive over regions of high refluxing (e.g., over hotter WPs) rather than over regions of low refluxing (e.g., over cooler WPs). Thus, variation in the spatial flux conditions caused by heating heterogeneity is potentially further increased by geochemical changes. These considerations emphasize the importance of considering geochemical changes when evaluating the performance implications of different engineering designs.

ACKNOWLEDGMENTS

We gratefully acknowledge the assistance of Sabrina Fletcher and Ron Shaffer in developing the graphics and of Karen L. Lew in editing and preparing this report. Discussions with George Barr, James W. Johnson and Nina Rosenberg were helpful. Work performed under the auspices of the U.S. Department of Energy by Lawrence Livermore National Laboratory under Contract W-7405-ENG-48.

REFERENCES

1. H.P. Taylor in *Geochemical Transport and Kinetics*, edited by A.W. Hofmann, B.J. Giletti, H.S. Yoder, Jr., and R.A. Yund (Carnegie Inst. Wash. Publ. 64, Washington, D.C., 1974), p. 299–324.

2. D. Norton, *Amer. J. Sci.* **288**, p. 604–618 (1988).

3. J.M. Ferry and G.M. Dipple, *Amer. Min.* **77**, p. 577–591 (1992).

4. N.D. Rosenberg, F.J. Spera, and R.M. Haymon, *Earth Planet. Sci. Lets*. **116**, p. 135-153 (1993).

5. T.A. Buscheck, in *Near-Field/Altered Zone Models Report* (Lawrence Livermore National Laboratory, UCRL-ID-129179, Livermore, CA, 1998), p. 3-1–3-91.

6. D. Norton and R. Knapp, *Amer. J. Sci.* **277**, p. 913–936 (1977).

7. J.W. Johnson, K.G. Knauss, W.E. Glassley, and L.D. DeLoach, *J. Hydrology* (1998) in press.

8. W.E. Glassley, *Coupled hydrogeochemical processes and their significance for Yucca Mountain Site Characterization* (UCRL-JC-114783, Lawrence Livermore National Laboratory, Livermore, CA, 1993).

9. J.J. Nitao, *Reference Manual for the NUFT Flow and Transport Code, Version 1.0.* (UCRL-IC-113520, Lawrence Livermore National Laboratory, Livermore, CA, 1995).